Proc. Natl. Acad. Sci. USA
Vol. 88, pp. 6018–6022, July 1991
Biochemistry

A β subunit mutation disrupting the catalytic function of *Escherichia coli* RNA polymerase

(abortive initiation/promoter clearance/pausing/elongation rate)

JOOKYUNG LEE*, MIKHAIL KASHLEV†, SERGEI BORUKHOV*, AND ALEX GOLDFARB*‡

*Department of Microbiology, Columbia University College of Physicians and Surgeons, New York, NY 10032; and †Institute of Molecular Genetics, U.S.S.R. Academy of Sciences, Moscow, U.S.S.R.

Communicated by E. Peter Geiduschek, March 25, 1991 (received for review February 13, 1991)

ABSTRACT **The substitution of the evolutionarily conserved Glu-813 for lysine in the β subunit of RNA polymerase (RNAP) causes a partial loss of function in the assembled RNAP. In the presence of the four ribonucleoside triphosphates, the mutant RNAP displayed a decreased frequency of promoter clearance and diminished elongation rate. Both defects could be compensated by raising the ribonucleoside triphosphate concentration. In the abortive initiation reaction limited by the incomplete set of ribonucleoside triphosphates, the mutant RNAP generated aberrant patterns of products indicative of their enhanced loss from the RNAP–promoter complex. A model is proposed, attributing the multiple effect of the mutation to the malfunctioning of the RNAP active center.**

RNA polymerase (RNAP) of *Escherichia coli* is a multifunctional multisubunit enzyme performing principal reactions of gene expression (1, 2). A key step of its functional cycle is the transition from the initial transcribing complex (ITC) to the elongating complex (EC) (3), also called "promoter clearance." In the ITC, the $\alpha_2\beta\beta'\sigma$ holoenzyme is stably anchored at the promoter, continuously making and releasing nested RNA oligomers, up to 9 nucleotides (nt) in length, in repeated acts of abortive initiation (3–7). Promoter clearance involves the release of the σ factor, relinquishing of the anchoring contacts, stabilization of the RNA product in the ternary complex, and commencement of processive elongation by the core enzyme $\alpha_2\beta\beta'$ (3, 7–9). The propagation of EC along the template occurs in rapid bursts punctuated by "pausing" at specific sites (10–13). Abortive initiation and pausing are probably linked to the catalytic mechanism of RNAP because their kinetic parameters are influenced by the concentration of ribonucleoside triphosphates (rNTP).

We have developed a method of probing RNAP vital features with transdominant mutations that lead to partial loss of function (14, 15). Here we characterize a single amino acid substitution in the β subunit, Glu-813 → Lys (E813K), which simultaneously accelerates oligomer loss at the ITC step, enhances pausing at the EC step, and decreases the frequency of ITC/EC transition, apparently through the disruption of the enzyme's active center.

MATERIALS AND METHODS

Genetic Techniques. The plasmids pXT7β, its *rpoB1855*-carrying derivative pJL97 (16), and pMKA92 (14) were described. pMKA351, pMKA335, and pMKA312 were isolated in the course of linker-insertion mutagenesis of pMKA92 (M.K., unpublished observations). For mapping of the mutation (Fig. 1*A*), donor pJL97 DNA was digested with appropriate restriction endonucleases to generate fragments F1, F2, F3, or F4. The recipient plasmids pMKA351, pMKA335, or pMKA312 were digested with the same endonucleases completely or (for *Pst* I) partially to generate appropriate targets for the insertion of each fragment. The donor and the recipient digests were ligated, digested with *Hin*dIII and *Bam*HI to eliminate the parental plasmids, and transformed into the HB101[pLacI^Q] host (14). For fragments F1, F2, and F3, successful fragment exchange was confirmed by the appearance of inducible full-sized β polypeptide due to the replacement of the *Bam*HI frameshifting linker of the recipient plasmid. To determine the genetic makeup of the recombinant plasmids the transformants were plated with and without Rif in the absence and in the presence of isopropyl β-D-thiogalactoside. For sequence determination, the fragment F2 (Fig. 1*A*) was inserted in both orientations into the *Pst* I site of the multiple cloning site of the M13mp19 vector. The directly oriented M13 insert was sequenced in the upstream direction from the distal *Pst* I site. The inversely oriented M13 insert was shortened by generating the *Hpa* I/*Sma* I deletion using the *Sma* I site within the vector sequence. The resulting clone was sequenced in the downstream direction from the *Hpa* I site in *rpoB*.

Biochemical Techniques. RNAP was reassembled from individually overexpressed subunits as described (14, 15). The reassembled enzymes were titrated in a reaction (see below) on the T7 A1 promoter by measuring the formation of the abortive product **CpApU** from **CpA** (here and later boldface type designates the priming nucleotide) and [α-^{32}P]UTP, to determine the point of saturation of the template with the enzyme. Transcription reactions were performed in 10 μl of the reaction buffer (14) containing ≈0.1 pmol of the 130-base-pair-long DNA fragment carrying the phage T7 A1 promoter (a gift from H. Heumann, ref. 17) and a saturating amount (0.3–0.4 pmol) of reconstituted RNAP. RNAP was preincubated with DNA in the presence of 0.5 mM of the priming dinucleotide (**CpA** or **ApU** obtained from Sigma) for 15 min at 37°C, and the reactions were started by adding the substrate mixture. The composition and the final concentrations of rNTP as well as the source of radioactivity are indicated in figure legends. In some reactions, terminating 3′-deoxynucleoside triphosphate (Pharmacia) was included, as indicated. The reactions were allowed to continue for 15 min (unless indicated otherwise), stopped by adding ethylenediaminetetraacetate to the concentration of 50 mM, and the mixtures were applied directly to polyacrylamide/8 M urea gels (20% acrylamide/3% *N,N′*-methylenebisacrylamide), which were run and autoradiographed as described (14). The sequences of abortive oligonucleotides were determined by using UTP, CTP, GTP, and ATP as alternative

The publication costs of this article were defrayed in part by page charge payment. This article must therefore be hereby marked "*advertisement*" in accordance with 18 U.S.C. §1734 solely to indicate this fact.

Abbreviations: EC, elongating complex; rNTP, ribonucleoside triphosphate(s); ITC, initial transcribing complex; Rif, rifampicin; RNAP, RNA polymerase; nt, nucleotide(s); E813K, Glu-813 → Lys; RNAP^{813}, RNAP carrying E813K; RNAP^{WT}, wild-type RNAP.

‡To whom reprint requests should be addressed.

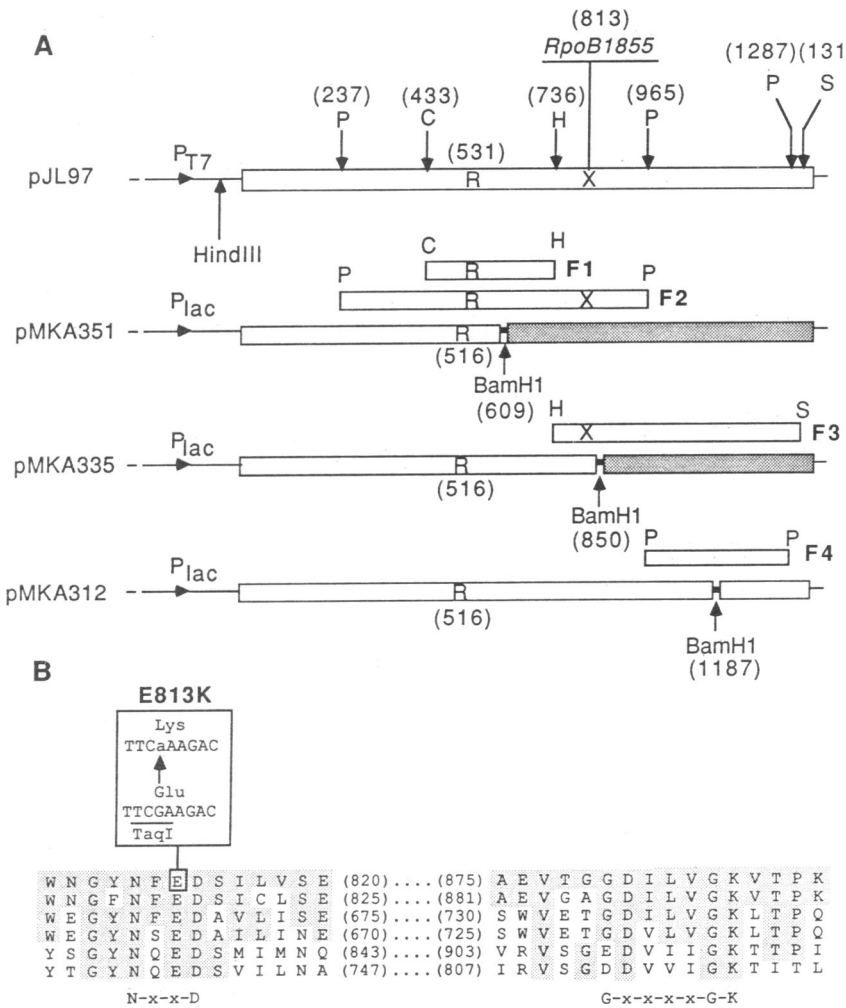

FIG. 1. *rpoB* mutation E813K (*rpoB1855*). (*A*) Localization of *rpoB1855* by transfer of the fragments F1, F2, F3, and F4 from plasmid pJL97 to one of the recipient plasmids of the pMKA series. Each recipient plasmid carries a *Bam*HI linker insertion (upward arrows) that inactivates β subunit function. For pMKA351 and pMKA335, the insertion causes the reading-frame shift (hatched areas). X and R designate the *rpoB1855* and a rifampicin (Rif)-resistance allele, respectively. P_{T7} and P_{lac} symbolize promoters. Restriction sites (downward arrows) are indicated as follows: P, *Pst* I; C, *Cla* I; H, *Hpa* I; and S, *Sma* I. Codon numbers are given in parentheses. The failure of recombinant plasmids to confer isopropyl β-D-thiogalactoside-dependent Rif resistance upon the host was taken as evidence that the transferred fragment carried the lethal *rpoB1855* mutation. (*B*) Sequence data and homology alignment. Nucleotide sequences around codon 813 are shown in the box with the mutant base set in lowercase. Amino acid sequences (from top to bottom) are from the β subunit of *E. coli* and from homologous segments of *Pseudomonas putida*, the chloroplasts of spinach and liverwort, *Saccharomyces cerevisiae*, and *Drosophila melanogaster*. Codon numbers are given in parentheses. Positions of identity to the *E. coli* sequence are screened. The putative nucleotide-binding motif (see *Discussion*) is shown underneath. These amino acid sequences are referenced elsewhere (14).

sources of the α-^{32}P label and by using terminating 3'-deoxyribonucleoside triphosphates. Transcripts were quantitated by cutting bands out of the gel slab and measuring the Cherenkov radioactivity.

To make synchronized stalled +20 complexes with RNAP carrying E813K ($RNAP^{813}$), the **ApU**-primed reaction was continued for 30 min with ATP and GTP (100 μM each) and 5 μM of [α-^{32}P]CTP. With wild-type RNAP ($RNAP^{WT}$), the **ApU**-primed reaction was carried out for 15 min with ATP, GTP, and [α-^{32}P]CTP (5 μM each). The reaction mixtures were then supplemented with RNase-free bovine serum albumin (Pharmacia) at 250 μg/ml and applied onto an FPLC Fast Desalting column (Pharmacia) equilibrated with 40 mM Tris, pH 7.9/60 mM NaCl. The UV-absorbing peak fraction was collected and stored at +4°C. To resume elongation, the samples were warmed to 37°C and supplemented with the missing components of the standard reaction containing either 5 μM or 50 μM of each of the four rNTP. Aliquots were withdrawn at time intervals, and then the reactions were stopped and analyzed in a 15% (acrylamide/*N,N'*-methylenebisacrylamide, 14:1) gel, as described above.

RESULTS

Mapping of *rpoB1855*. The mutation *rpoB1855* was originally isolated as a dominant lethal mutation, after random mutagenesis of the expression plasmid pXT7β, which carries a Rif-resistant allele of *rpoB* (16). To map *rpoB1855*, a series of *in vitro* exchanges of DNA fragments (F1, F2, F3, and F4) was performed between plasmids as illustrated in Fig. 1*A*. Using Rif resistance as the indicator of functionality of plasmid-encoded β, the mutation was mapped within the 697-bp overlap of fragments F2 and F3, between *Hap* I and *Pst* I restriction sites. This segment was sequenced in both orientations, and the mutation was found to be the substitution of Glu-813 for lysine (Fig. 1*B*, box).

E813K Inhibits Promoter Clearance. $RNAP^{813}$ holoenzyme carrying β subunit with the substitution was reconstituted from individually overexpressed subunits (14, 15). As the control, $RNAP^{WT}$ carrying the β subunit specified by the parent plasmid pXT7β was assembled. Both preparations contained nearly stoichiometric amounts of σ. However, $RNAP^{813}$ was totally inactive *in vitro* on T4 DNA as well as on several promoter DNA fragments, whereas $RNAP^{WT}$ displayed high specific activity. Yet, in all cases, $RNAP^{813}$ generated abortive oligomers with high efficiency (data not shown). Thus, $RNAP^{813}$ is qualitatively deficient in the promoter clearance step of the transcription cycle.

Fig. 2 presents the quantitation of this defect for the phage T7 A1 promoter. To limit transcription to a single round, the following scheme was used. The initial transcribed sequence of this promoter is **ApU**pCpGpA→, and the next uridine is located at position +21. The transcription was initiated with the dinucleotide **ApU**, whereas UTP was substituted with its chain-terminating analog 3'-deoxyuridine triphosphate. Under these conditions, EC is expected to propagate unimpeded until it stalls at position +21. Because each template fragment can accommodate only one stalled EC, the maximum number of stalled complexes formed at RNAP excess should be equal to the number of template molecules. The time needed to reach this maximum should reflect the rate of promoter clearance.

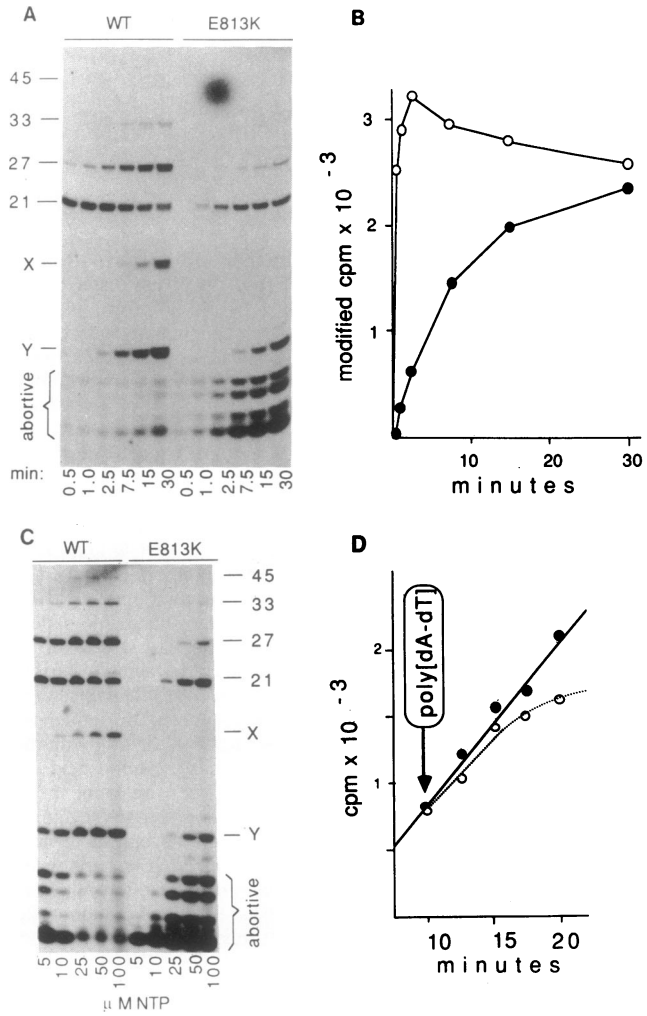

FIG. 2. Analysis of promoter clearance. (*A*) Time course of a single-round transcription reaction. RNA chains were initiated with **ApU** in the presence of ATP and GTP (0.1 mM each), 50 μM [α-^{32}P]CTP, and 0.5 mM of 3′-deoxyuridine triphosphate, at 3-fold molar excess of RNAP over template, and the reactions were stopped after indicated time intervals. Numbers 21, 27, 33, and 45 indicate length in nucleotides of the transcripts arrested within the A1 transcription unit. Unidentified abortive products are resolved at the bottom of the gel. Products X and Y are due to artifacts discussed in the text. (*B*) Quantitation of arrested EC. Cumulative radioactivity of bands 21 and 27 of *A*, expressed as modified cmp after correction for the number of labeled phosphates. Each point was obtained by adding the Cherenkov count of band 21 to two-thirds of the count of band 27 to account for the fact that the two transcripts contain 4 and 6 radioactive cytosine nucleotides, respectively. WT, open symbols; E813K, closed symbols. (*C*) Dependence of promoter clearance on substrate concentration in a single-round reaction. The **ApU**-primed reactions similar to those in *A* were incubated for 15 min with 0.5 mM of 3′-deoxyuridine triphosphate and the indicated concentrations of ATP, GTP, and [α-^{32}P]CTP, maintained at constant specific radioactivity. (*D*) Stability of E813K ITC. Time course of production of **CpApUpC** in the **CpA**-primed reaction with 100 μM UTP and 50 μM [α-^{32}P]CTP. Two parallel reactions were allowed to proceed for 10 min, after which poly[dA-dT] was added to one of them (open symbols) to the final concentration of 0.1 mg/ml. A control demonstrating instantaneous inactivation of free RNAP by poly[dA-dT] was performed (data not shown).

When this experiment was done (Fig. 2*A*), it was noted that the EC stalled not at one but at several points corresponding to uridine positions +21, +27, +33, and +45. We attribute this read-through phenomenon to pyrophosphorolysis and the presence of contaminating UTP in the commercial lots of other rNTP (18). The stalled EC could be chased to yield the 65-nt runoff transcript by adding large excess of natural UTP (data not shown). The two unexpected bands (X and Y in Fig. 2*A*) are attributed to artifacts. X represents a start site other than the A1 promoter, as was demonstrated by transcript mapping with restriction enzymes (data not shown). Y, which accumulated only under the conditions of arrested elongation, apparently represents the activity of secondary RNAP molecules binding at the vacated A1 promoter after the initial complexes have moved to position +27 and/or +33.

Quantitation of cumulative radioactivity in bands 21 and 27 of Fig. 2*A* is shown in Fig. 2*B*. Clearly, the accumulation of stalled EC in the RNAP^{WT} reaction (open symbols) was essentially complete between 0.5 and 1 min. For RNAP^{813} (closed symbols), the number of stalled EC approached a plateau only by 30 min. The level of this plateau was reproducibly at least three-quarters that of RNAP^{WT}, indicating that most available template fragments were eventually used by the RNAP^{813}. It should be noted that RNAP^{813} generated much more abortive oligomers per productive initiation than RNAP^{WT} (Fig. 2*A*). The use of the promoter by RNAP^{813} was not only slow but required unusually high concentrations of rNTP (Fig. 2*C*). At rNTP concentrations below 25 μM, few stalled EC were generated by RNAP^{813}, even after prolonged incubation, whereas RNAP^{WT} used the promoter with high efficiency in the rNTP concentration range from 5 to 100 μM.

The slow accumulation of EC can, in principal, be due to either premature dissociation of RNAP^{813} from the promoter or decreased rate of ITC → EC transition. The latter possibility seems more likely because of the effect of substrate concentration as well as the relative overproduction of abortive oligomers by RNAP^{813}. This explanation is reinforced by the experiment of Fig. 2*D*, in which the mutant catalytic ITC was challenged with DNA competitor poly[dA-dT] as it was producing the abortive tetramer **CpApUpC**. In this experiment, the −1,+1 primer **CpA** had to be used because **ApU** is complementary to poly[dA-dT]. The formation of chains longer than **CpApUpC** was prohibited because GTP and ATP

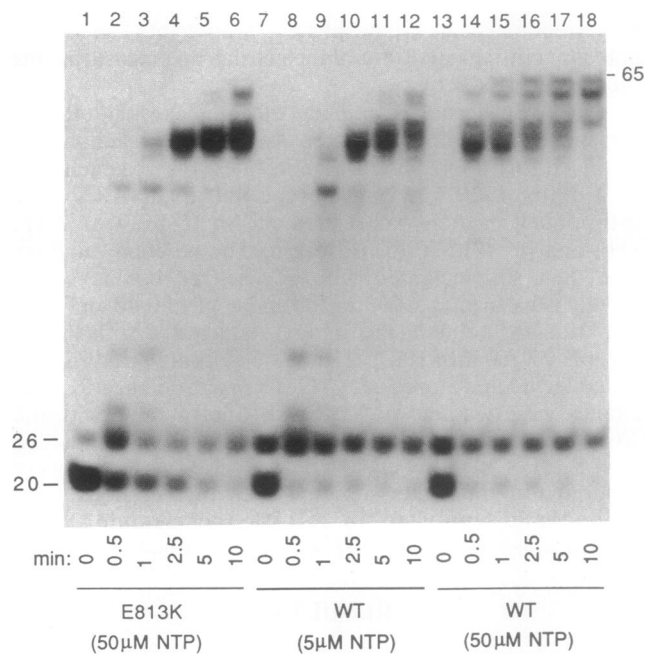

FIG. 3. Analysis of elongation. The EC complexes stalled at positions +20 and +26 (lanes 0) were purified from unincorporated rNTP by gel filtration. They were incubated with either 50 μM (lanes 1–6, 13–18) or 5 μM (lanes 7–12) of nonradioactive rNTP for indicated time periods under otherwise standard conditions. Position of the 65-nt runoff transcript is indicated.

were absent. It can be seen that after the addition of the competitor the catalytic reaction slowed down with an apparent half-life of ≈10 min. A similar level of poly[dA-dT] resistance was seen during catalytic pentamer (**CpA**pUpCpG) formation. Thus, although the mutant ITC is less stable than the wild-type complex that was totally poly[dA-dT] resistant (data not shown), ITC dissociation cannot account for the dramatic inhibition of the initiation rate observed, especially at suboptimal substrate concentrations. We conclude that the principal deficiency of $RNAP^{813}$ is in the ITC/EC transition.

E813K Slows Elongation. We next compared the elongation rate (and its dependence on rNTP concentration) of the E813K and wild-type EC that were synchronized at position +20 by omitting UTP from the initial reaction mixture and then purified by gel filtration (Fig. 3). When the isolated stalled EC (lanes 1, 7, and 13) were allowed to resume elongation by the addition of the four standard rNTP, a dramatic difference between $RNAP^{813}$ (lanes 1–6) and $RNAP^{WT}$ (lanes 7–18) was observed. With $RNAP^{813}$ almost no chain extension was evident at 5 μM of rNTP (data not shown), whereas it took 10 times higher concentration of rNTP (50 μM, lanes 1–6) to achieve the elongation rate and the pausing pattern seen at 5 μM rNTP with $RNAP^{WT}$ (lanes 7–12). Under the same rNTP concentration (50 μM rNTP), $RNAP^{WT}$ and $RNAP^{813}$ synthesized chains of comparable length after 30 sec (lane 14) and 10 min (lane 6), respectively.

Aberrant Abortive Initiation by $RNAP^{813}$. That the promoter clearance and elongation defects of $RNAP^{813}$ could be compensated by excess rNTP suggests that the mutation may have affected the catalytic function of the enzyme. To explore this possibility, we analyzed in more detail abortive initiation (Fig. 4 *A* and *B*). In this experiment, RNA chains were primed with **CpA** corresponding to the initial transcribed sequence **CpA**pUpCpGpApG→. To prevent promoter clearance, 3′-deoxy analogs of GTP (*A*) and ATP (*B*), which terminate chains at positions +4 and +5, respectively, were added. RNAP was in excess, thus limiting the maximum number of catalytic complexes to the number of available promoters. The assays were done in the absence of DNA competitors, allowing an average mutant RNAP to dissociate and rebind once per 15 min of the steady-state reaction (based on the 10-min complex half-life, see Fig. 2*D*). Fig. 4*C* presents the control multiple-round reaction containing the four natural rNTP, in which promoter clearance was allowed to occur.

In the "+4" reaction (Fig. 4*A*), the pentamer **CpA**pUpCpG was the predominant product of $RNAP^{WT}$. By contrast, $RNAP^{813}$ also generated **CpA**pU in substantial amounts. Furthermore, the total production of oligomers by $RNAP^{813}$ was ≈three times higher than by $RNAP^{WT}$. This result could not reflect a larger number of active complexes because the number of available promoters was the limiting factor. Moreover, as was shown above (see Fig. 2 *A* and *B*), the number of productive complexes was in fact slightly lower in the $RNAP^{813}$ than in the wild-type reaction. Thus, the enhanced productivity of $RNAP^{813}$ can be explained only by faster catalytic rate of the mutant complexes.

In the "+5" reaction (Fig. 4*B*), the higher overall initiation rate and the generation of trimer **CpA**pU by $RNAP^{813}$ were again evident. However, the hexamer **CpA**pUpCpGpA was dramatically underproduced by $RNAP^{813}$. The production of **CpA**pUpCpGpA by $RNAP^{813}$ could be brought to the wild-type level by increasing the ATP concentration ≈10-fold (compare 50 μM WT and 500 μM E813K lanes). Under these conditions, production of the pentamer **CpA**pUpCpG by $RNAP^{813}$ was at least three times higher than by $RNAP^{WT}$. Thus, the efficiency of extension of **CpA**pUpCpG to **CpA**pUpCpGpA is inhibited by the mutation ≈30-fold. In conclusion, the abortive initiation reaction performed by $RNAP^{813}$ reveals two distinct characteristics of the mutant ITC: a faster catalytic rate with regard to the shorter abortive products and a strong barrier in extending RNA chains between the +4G and +5A positions of the initial transcribed sequence.

DISCUSSION

The substitution E813K causes multiple functional changes in RNAP. $RNAP^{813}$ was found to have (*i*) a qualitatively different

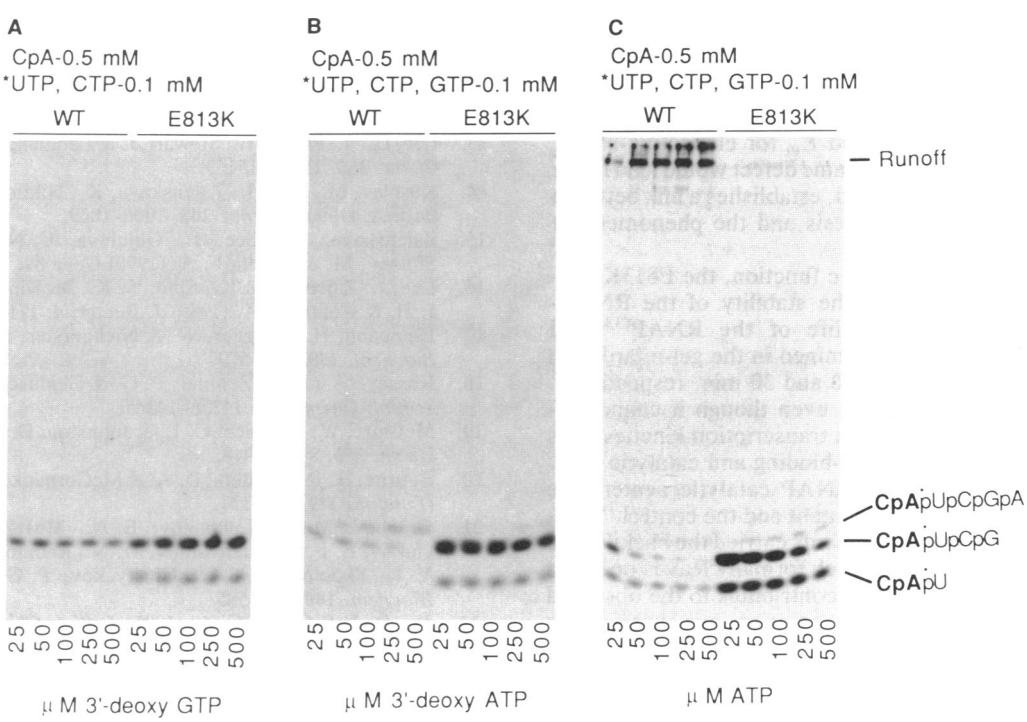

FIG. 4. Analysis of abortive initiation. Comparison of the $RNAP^{WT}$ and $RNAP^{813}$ in the standard *in vitro* assay with (*A* and *B*) or without (*C*) chain-terminating nucleotides. 3′-deoxy GTP, 3′-deoxyguanine triphosphate; 3′-deoxy ATP, 3′-deoxyadenosine triphosphate.

pattern of abortive products, (*ii*) a diminished frequency of the ITC → EC transition, and (*iii*) an enhanced pausing. The decrease in promoter clearance (30 min vs. 30 sec in the single-round reaction of Fig. 2 *A* and *B*) and the elongation slowdown were sufficient to bring transcription in the multiple-round reaction to almost a total halt (Fig. 4*C*).

The effect on promoter clearance and the apparent prolongation of pausing can be compensated by higher rNTP concentration. Hence, both defects could be from a decreased affinity for the elongation substrate. This explanation, however, does not fit the observed changes in the abortive reaction. For example, the enhanced production of **CpA**pUpCpG and the formation of **CpA**pU by RNAP^{813} (Fig. 4*A*) cannot be explained by a reduced binding of rNTP. Similarly, RNAP^{813} and RNAP^{WT} generated **CpA**pUpCpGpA with the same rate at 500 μM and 50 μM ATP, respectively (Fig. 4*B*). If the substrate binding were the only defect, under these conditions the two enzymes should have produced the shorter oligomers at the same rate. In reality, RNAP^{813} dramatically overproduced **CpA**pUpCpG and **CpA**pU, which contradicts the notion of a decreased affinity for rNTP.

We propose that the primary effect of the mutation is a destabilization of the nascent RNA product in the active center. Assuming that the rate of abortive initiation is limited by the release of **CpA**pUpCpG, the enhanced loss of this product from the mutant ITC would lead to more frequent initiation. The accumulation of **CpA**pU is explained by the loss of a fraction of this product before it gets extended with the next nucleotide. The kinetic barrier for **CpA**pUpCpG extension to **CpA**pUpCpGpA is explained by an exceptionally high K_m of this step even with RNAP^{WT}. The combined effect of the accelerated oligomer release and a high K_m of a distal step of the abortive reaction explains how the mutation may inhibit promoter clearance, especially if a high K_m step is repeated more than once in the initial transcribed sequence. In accord with this model, RNAP^{813} displayed diminished yield of longer abortive oligomers also in reactions primed with **ApU** (Fig. 2*C*) as well as with several other promoters (data not shown).

The effect of E813K on elongation can be explained in the same vein, assuming that the binding site for the incoming (elongating) substrate is formed, in part, by the nascent 3′ RNA terminus (19). If the mutation affects the holding of the 3′ terminus, the prevailing consequence for the intrinsically stable EC would be an increased K_m for elongating rNTP, whereas in the unstable ITC the same defect would lead to the oligomer loss. This model, if valid, establishes a link between the catalytic act of RNA synthesis and the phenomena of abortive initiation and pausing.

Besides disrupting the catalytic function, the E813K substitution somewhat decreases the stability of the RNAP–promoter complex. The half-life of the RNAP^{813} and RNAP^{WT} open complexes determined in the gel-retardation assay (data not shown) was ≈10 and 30 min, respectively. This difference is worth noting, even though it cannot account for the observed defects in transcription kinetics. It is not inconceivable that the DNA-binding and catalytic functions partially overlap in the RNAP catalytic center. We should also note that both the mutant and the control "wild-type" RNAP used in our experiments carried the background Rif-resistant marker *RifD18*, which formally leaves open the possibility that the Rif mutation contributes to the observed RNAP^{813} properties. With this reservation, our observations are pertinent to the role of the Glu-813 residue in the RNAP molecule. It is tempting to speculate that Glu-813 directly contacts the RNA product in the active center. In this connection, we note that Glu-813 is a member of a conserved bipartite nucleotide binding motif N-x-x-D. . .G-x-x-x-x-G-K (Fig. 1*B*) which is found in many GTP- and ATP-binding proteins (20).

So far chemical and genetic data have implicated other localities of the β polypeptide in the catalytic function. Crosslinking experiments (21) and site-directed mutagenesis (14) have positioned Lys-1065 and His-1237 in close vicinity to the priming nucleotide. RNAP from the Rif-resistant mutant *rpoB8* (Gln-513 → Pro) revealed a changed K_m for purine nucleotides during elongation (22). Systematic mutational analysis of these localities will help to clarify their roles and relationship to each other.

We are grateful to Katya Zalenskaya for advice on RNAP reconstitution and to Vadim Nikiforov, Michael J. Chamberlin, and George Kassavetis for discussion and criticism. This work was supported by grants from the National Institutes of Health (GM30717) and the American Cancer Society (MV-285). M.K. was a recipient of the Soros Foundation–Soviet Union Travel Fellowship.

1. von Hippel, P. H., Bear, D. G., Morgan, W. D. & McSwiggen, J. A. (1984) *Annu. Rev. Biochem.* **53**, 389–446.
2. McClure, W. R. (1985) *Annu. Rev. Biochem.* **54**, 171–204.
3. Krummel, B. & Chamberlin, M. J. (1989) *Biochemistry* **28**, 7829–7842.
4. Johnston, D. E. & McClure, W. R. (1976) in *RNA Polymerase*, eds. Losick, R. & Chamberlin, M. (Cold Spring Harbor Lab., Cold Spring Harbor, NY), pp. 101–126.
5. Carpousis, A. J. & Gralla, J. D. (1980) *Biochemistry* **19**, 3245–3253.
6. Levin, J. R., Krummel, B. & Chamberlin, M. J. (1987) *J. Mol. Biol.* **196**, 85–100.
7. Hansen, U. M. & McClure, W. R. (1979) *J. Biol. Chem.* **254**, 5713–5717.
8. Straney, D. C. & Crothers, D. M. (1987) *J. Mol. Biol.* **193**, 267–278.
9. Metzger, W., Schikor, P. & Heumann, H. (1989) *EMBO J.* **8**, 2745–2754.
10. Maizels, M. (1973) *Proc. Natl. Acad. Sci. USA* **70**, 3585–3589.
11. Kassavetis, G. A. & Chamberlin, M. J. (1981) *J. Biol. Chem.* **256**, 2777–2786.
12. Arndt, K. M. & Chamberlin, M. J. (1990) *J. Mol. Biol.* **213**, 79–108.
13. Lee, D. N., Phung, L., Stewart, J. & Landick, R. (1990) *J. Biol. Chem.* **265**, 15145–15153.
14. Kashlev, M., Lee, J., Zalenskaya, K., Nikiforov, V. & Goldfarb, A. (1990) *Science* **248**, 1006–1009.
15. Zalenskaya, K., Lee, J., Gujuluva, C. N., Shin, Y. K., Slutsky, M. & Goldfarb, A. (1990) *Gene* **89**, 7–12.
16. Lee, J., Zalenskaya, K., Shin, Y. K., McKinney, J. D., Park, J. H. & Goldfarb, A. (1989) *J. Bacteriol.* **171**, 3002–3007.
17. Heumann, H., Metzger, W. & Niehoerster, M. (1986) *Eur. J. Biochem.* **158**, 575–579.
18. Kassavetis, G. A., Zentner, P. G. & Geiduschek, E. P. (1986) *J. Biol. Chem.* **261**, 14256–14265.
19. McClure, W. R., Cech, C. L. & Johnston, D. E. (1978) *J. Biol. Chem.* **253**, 8941–8948.
20. Bourne, H. R., Sanders, D. A. & McCormick, F. (1991) *Nature (London)* **349**, 117–127.
21. Grachev, M. A., Lukhanov, E. A., Mustaev, A. A., Zaychikov, E. F., Abdukayumov, M. N., Rabinov, I. V., Richter, V. I., Skoblov, Y. S. & Chistyakov, P. G. (1989) *Eur. J. Biochem.* **180**, 577–585.
22. Jin, D. J. & Gross, C. A. (1991) *J. Biol. Chem.* in press.